LAWRENCE
LIVERMORE
NATIONAL
LABORATORY

LLNL-TR-743973

Collaborative, Nondestructive Analysis of Contaminated Soil

K. B. Knight, Z. Dai, L. Davidson, G. Eppich, R. Lindvall, T. Parsons-Davis, C. Ramon, S. Roberts, M. Sharp, H. J. Turin, S. LaMont, T. Zidi, M. Belamri, S. Bounatiro, S. Benbouzid, A. S. Fellouh, T. Idir, Y. Larbah, M. Moulay, A. Noureddine, B. Rahal

January 4, 2018

Disclaimer

This work performed under the auspices of the U.S. Department of Energy by Lawrence Livermore National Laboratory under Contract DE-AC52-07NA27344.

Collaborative, Nondestructive Analysis of Contaminated Soil

Lawrence Livermore National Laboratory (LLNL)

K.B. Knight, Z. Dai, L. Davisson, G. Eppich, R. Lindvall, T. Parsons-Davis, C. Ramon, S. Roberts, M. Sharp

Los Alamos National Laboratory (LANL)

H.J. Turin, S. LaMont

Commissariat á l'Energie Atomique (COMENA)

T. Zidi, M. Belamri, S. Bounatiro, S. Benbouzid, A.S. Fellouh, T. Idir, Y. Larbah, M. Moulay, A. Noureddine, B. Rahal

December 1, 2017

Disclaimer

Auspices Statement

This work performed under the auspices of the U.S. Department of Energy by Lawrence Livermore National Laboratory under Contract DE-AC52-07NA27344.

1. Summary

This report summarizes a joint nondestructive analysis exercise that LLNL, LANL, and COMENA discussed through a collaborative meeting in July 2017. This work was performed as one part of a collaboration with Algeria under Action Sheet 7: "Technical Cooperation and Assistance in Nuclear Forensics". The primary intent of this exercise was for US and Algerian participants to jointly share results of nondestructive analyses (NDA) of a contaminated soil sample provided by the Algerians and to discuss key observations and analytical approaches. While the two samples were analyzed blind at LLNL and LANL, the soil samples were revealed after the exercise to have a common origin, and to have originated as an IAEA soil sample (IAEA-326, Bojanowski *et al.*, 2001) provided to COMENA as part of a previous exercise. Comparative analysis revealed common findings between the laboratories, and also emphasized the need for standardized operating procedures to improve inter-comparability and confidence in conclusions. Recommended handling practices in the presence of sample heterogeneities were also discussed.

This exercise provided an opportunity to demonstrate nuclear forensics analytical capabilities at COMENA, LANL, and LLNL, and identified areas that could benefit from future technical exchanges. Plans were made for a follow-on joint exercise in 2018, involving destructive analyses of the CUP-2 uranium ore concentrate standard.

2. Introduction

This report documents nondestructive analyses conducted on a soil sample jointly analyzed by Algerian Commissariat á l'Energie Atomique (COMENA), Lawrence Livermore National Laboratory (LLNL), and Los Alamos National Laboratory (LANL). The science of Nuclear Forensics has been developing over the last two decades with substantial contributions from a number of institutions (*e.g.*, Moody *et al*., 2005; Mayer *et al.*, 2013). The practice of Nuclear Forensics requires a sustainable infrastructure with personnel actively engaged in nuclear measurements, laboratories with dedicated instrumentation, and continued practice and experience gained by making measurements on mock or actual Nuclear Forensic materials. It is because of this latter requirement that experienced institutions collaborate with international counterparts to help build and sustain the capacity to handle actual Nuclear Forensic materials. Participating in joint measurement exercises is an essential step to demonstrating and evolving this expertise. It is the intent of this paper to present measurements made by each institution, provide comparative observations, and document insights gained.

3. Sample Receipt, Preliminary Measurements, and Aliquoting

COMENA selected an in-house soil sample for comparative measurements with LLNL and LANL. The two samples provided to LLNL and LANL were analyzed blind, and not presumed *a priori* to be related. The soil samples were revealed after the exercise to have a common origin, originating from an aliquot of an IAEA soil sample (IAEA-326, Bojanowski *et al.*, 2001) provided to COMENA as part of a previous exercise.

At COMENA ~250 g was separated from the original, parent sample, which was in a ground and powdered format. Two sub-aliquots of ~15 g each were separated and provided to LLNL. A sub-aliquot of ~10 g was provided for multiple analyses at COMENA, and the remaining ~100 g was used for γ-spectrometry analyses at COMENA.

Two plastic vials were received at LLNL, where they were labeled NSDD-16-1 and NSDD-16-2. The vials arrived in a plastic container with a lid, inside of a cardboard shipping box. Each vial was confirmed to weigh approximately 15 grams. Each vial was placed individually into a Canberra model BE5025 HPGe gamma spectrometer and counted for 24 hours, 4 centimeters from the detector. This preliminary analysis detected the presence of ^{137}Cs in both samples, along with the natural radioactive nuclides of ^{40}K, ^{226}Ra, ^{228}Ra, ^{212}Pb, and ^{208}Tl (*see* Table 1). No transuranic actinides were detected by this survey measurement, though the daughter products of natural uranium decay were observed.

Table 1. Preliminary 24-hour gamma spectrometry results (LLNL). Measurement uncertainties are 2σ.

	NSDD-16-1	
Nuclide	Activity (pCi)	Uncertainty
^{137}Cs	36	4
^{40}K	223	33
^{226}Ra	14	2
^{228}Ra	16	3
^{212}Pb	20	2
^{208}Tl	5	1
	NSDD-16-2	
Nuclide	Activity (pCi)	Uncertainty
^{137}Cs	34	3
^{40}K	198	27
^{226}Ra	13	1
^{228}Ra	18	5
^{212}Pb	18	1
^{208}Tl	5	1

After preliminary γ-spectrometry at LLNL, the vials were opened individually to avoid cross-contamination and inspected visually. Preliminary visual inspection showed both samples to be dark grey, fine-grained powders (*see* Fig. 1). Due to dispersion and cross-contamination concerns, the two samples were not handled concurrently. The two LLNL samples were transferred to new, clean vials and weighed (NSDD-16-1 = 14.915 ± 0.001 g; NSDD-16-2 = 14.914 ± 0.001 g). Sub-aliquots (between 4-6 g) were then removed from each vial, placed in separate containers, and shipped to LANL for analysis. Sub-aliquot IDs and masses are listed in Table 2.

Figure 1. Optical images of the two aliquots as received at LLNL. The image at right shows the fine, dark grey form of the powered material, which was similar between the two samples.

4. Analytical Planning

All three labs conducted gamma spectrometry on sample aliquots to determine the presence and concentrations of γ-emitting radionuclides. LLNL and COMENA also performed X-ray diffraction (XRD) to identify crystalline phases, X-ray fluorescence (XRF) to determine elemental composition, and scanning electron microscopy (SEM) to establish physical form and dimensions. In addition, LLNL performed optical characterization, autoradiography, and alpha spectrometry. While the latter is not a technically a nondestructive analysis, it has been included in this report for completeness.

Table 2. Sub-aliquot IDs and recorded masses (g) for individual measurements at LLNL and LANL, errors on masses are ± 0.001 g.

Sample ID	Aliquot	Mass (g)
NSDD-16-1	As received	14.915
NSDD-16-2	As received	14.914
NSDD-16-1-1	LLNL Aliquot	9.069
NSDD-16-2-1	LLNL Aliquot	10.992
NSDD-16-1-2	LANL Aliquot	5.846
NSDD-16-2-2	LANL Aliquot	3.922
NSDD-16-1-1-A	Alpha Spectrometry	0.818
NSDD-16-2-1-A	Alpha Spectrometry	1.312
NSDD-16-1-1-B	XRF/XRD/Autorad	0.45
NSDD-16-2-1-B	XRF/XRD/Autorad	0.494
NSDD-16-1-1-C	Microscopy	trace
NSDD-16-2-1-C	Microscopy	trace
NSDD-16-1-1-D	Gamma Spec/Archive	7.801
NSDD-16-2-1-D	Gamma Spec/Archive	9.185

5. Optical Inspection

The two samples retained at LLNL (NSDD-16-1-1 and NSDD-16-2-1) were visually inspected to determine the degree of uniformity of the material and to enable inter-comparison of the two samples. Optical imaging of the samples confirmed both powders to be fine-grained powder of

similar grey-brown color (*see* Fig. 2). The samples were dry and dispersed easily, with no significant moisture content. No heterogeneities were observed within either powder, and samples in the two vials were indistinguishable based on optical inspection. Following optical inspection, the LLNL samples were further sub-aliquoted, as noted in Table 2.

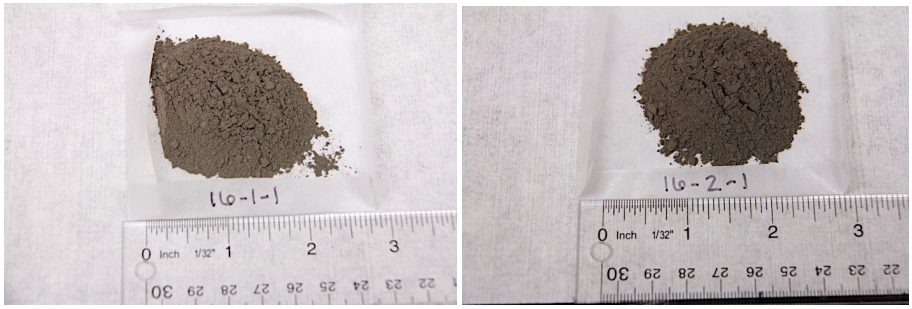

Figure 2. Optical inspection of the two aliquots retained at LLNL. No differences were noted between the samples, and no heterogeneities were observed at this scale.

6. Autoradiography

Autoradiography is a qualitative nondestructive method that can image the 2-dimensional spatial distribution and relative intensity of radioactivity in a powdered or solid sample (Parsons-Davis *et al.*, submitted). The sample is placed in contact with an image plate and the energetic particles generated in radioactive decay produce an image by photo-stimulated luminescence. In the case of soil samples and other types of particulate samples, images can reveal the presence of individual hot particles, in contrast with conventional counting methods such as γ, α, or β^- spectrometry that characterize the average characteristics of the bulk sample.

Figure 3. Images of the sample-loaded Gel Pak boxes used for obtaining autoradiographs of the two samples provided to LLNL. Grids are 8.5 x 5.5 cm.

To obtain autoradiographs, sub-aliquots of the two samples (NSDD-16-1-1-B and NSDD-16-2-1-B) were dispersed as a thin layer onto an adhesive Gel Pak box across an 8.5 x 5.5 cm grid pattern (Fig. 3). A super resolution (SR) phosphor image plate, emulsion side down, was placed over top of the loaded grids with lead weights to secure it in place. The Gel Pak boxes were then closed and placed in a dark tent for 4 weeks. Image plates were recovered and imaged using a General Electric Typhoon FLA 7000 scanner at 1000 V. Images were processed with the program ImageJ.

Images revealed no significant detection of alpha or beta activity in either dispersion. Background detection of natural cosmic or terrestrial radioactivity, however, was visible on developed images. On average, this background signal was higher outside the regions shielded by the Pb weight (which included areas in contact with the soil samples), suggesting very low radioactivity in the samples (Fig. 4).

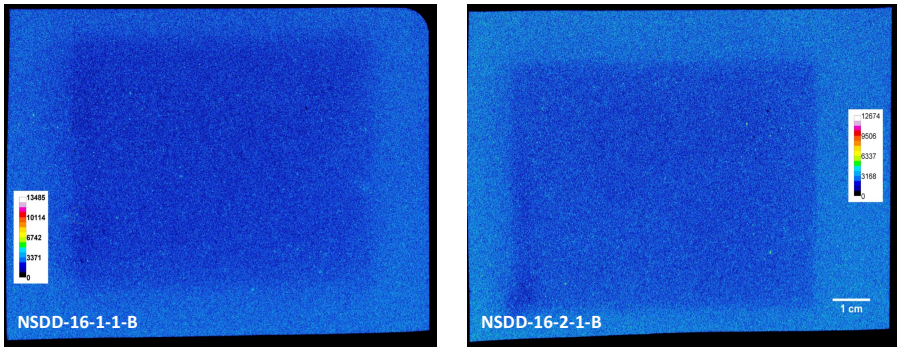

Figure 4. Autoradiographs of the two sample aliquots at low resolution, illustrating the impact of cosmic ray and other background, and the low radioactivity of the soil. No significant differences can be observed between the two sample images.

Low-resolution images suggest that trace amounts of radioactivity are present in both samples, but this activity is likely heterogeneously distributed as hot particles. This hypothesis required additional imaging and processing for confirmation. The images have a 25 µm pixel size and overal spatial resolution of approximately ~50 µm, thus imaging software can enable analysis at multiple scales. Areas where hot particles were suspected were enlarged, and the local intensity reconstructed as a 3-dimensional image (Fig. 5). Based on these analyses, the spatial heterogeniety is consistent with the presence of hot particles in both of the samples and constitues the majority of the overall radioactivity of the samples. However, the small grain size of the powder in combination with the low radioactivity make it difficult to definitively attribute “hot spots” to specific particles. It was discussed that use of external shielding to lower background interferences may help reduce backgrounds in future, similar analyses.

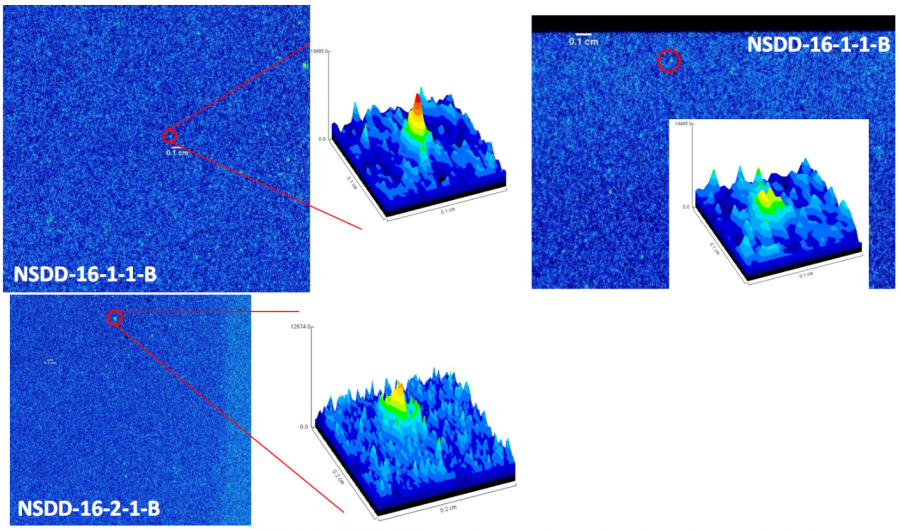

Figure 5. Enlarged images rendered as 3-D intensity maps of suspected hot particles in the two samples (left) illustrate high intensity 'hot spots' ranging in dimension from approximately 100 to 500 microns. The upper right image illustrates the ambiguity with a "hot spot" from outside of the shielded sample region, presumably caused by background radiation.

7. X-ray Diffraction

Powder XRD can identify crystalline phases present in a sample and determine their ratios quantitatively. The technique involves directing a beam of X-rays onto a sample and observing the scattering angles caused by X-ray interactions with atomic lattices. Powder XRD patterns of various materials have been compiled over many decades, and XRD data from a given sample are generally interpreted through comparison with an XRD library to identify the crystalline phases present in the sample.

LLNL's method for XRD analyses of bulk powder samples calls for drying an alcohol slurry of the sample on a zero-background silicon plate embedded in a polymethyl methacrylate (PMMA) sample holder. Samples were analyzed on a Bruker AXS D8 ADVANCE X-ray diffractometer equipped with a LynxEye 1-dimensional linear Si strip detector. Operating parameters included a Ni-filtered Cu radiation from a sealed tube at 40 kV and 40 mA. Scan parameters were 10° to 70° 2θ, with a 0.02° step, 3 second dwell time, and 6 mm divergence slit. Raw data were processed with DIFFRAC.EVA V3.1 software. X-ray reference material (Al_2O_3) was analyzed with the sample to ensure goniometer alignment. No peak shift in the standard scan was observed when the sample was analyzed. Phases were identified by peak comparison with ICDD PDF-2 2009 and PDF-4+ 2014 powder diffraction databases. Table 3 lists the identified phases from the XRD analysis. A comparison of the results from the 2 samples reveals several apparent differences:

microcline makes up 10% of sample 2 but is missing in sample 1, while orthoclase makes up 6.5% of sample 1 and is absent from sample 2. Albite and anorthite are closely related minerals in the plagioclase family of feldspars, and microcline and orthoclase are closely related potassium feldspar minerals ("K-spar"). If these mineral families are considered, sample 1 (80% quartz, 11% plagioclase, 7% K-spar) and sample 2 (76% quartz, 12% plagioclase, 10% K-spar) are quite similar.

Table 3. Phases identified by XRD analysis, and their relative abundances (LLNL).

		NSDD-16-1-1-B	
Pattern #	**Compound**		**Abund.**
00-046-1045	Quartz	SiO_2	79.7%
04-017-0892	Albite, calcic	$Na_{0.84}\ Ca_{0.16}\ Al_{1.16}\ Si_{2.84}\ O_8$	10.8%
00-008-0048	Orthoclase	$K\ (Al\ ,\ Fe)\ Si_2\ O_8$	6.5%
00-006-0158	Chloritoid	$(Fe,\ Mg)_2\ Al_4\ Si_2\ O_{10}\ (O\ H)_4$	3.0%
		NSDD-16-2-1-B	
Pattern #	**Compound**	**Formula**	**Abund.**
00-046-1045	Quartz	SiO_2	76.1%
01-083-1895	Microcline	$K_{0.96}\ Na_{0.04}\ Al\ Si_3\ O_8$	9.9%
04-017-0892	Albite, calcian	$Na_{0.84}\ Ca_{0.16}\ Al_{1.16}\ Si_{2.84}\ O_8$	6.9%
01-076-0832	Anorthite, sodic	$(Ca_{0.86}\ Na_{0.14})\ (Al_{1.84}\ Si_{2.16}\ O_8)$	5.2%
00-002-0009	Montmorillonite	$Si_{3.74}\ Al_{2.03}\ Fe_{0.03}\ Mg_{0.02} \cdot O_{11}$	1.5%
03-065-5714	Anatase	TiO_2	0.5%

COMENA's methods for XRD analysis entailed cleaning the sample holder with ethanol, then placing the soil powder into the sample holder, wetting the sample, and compacting it to produce a thin layer with a flat surface. The diffractometer was calibrated using silicon, followed by insertion of the sample. Analyses were performed on a Phillips XPert Pro equipped with a Cu X-ray source operated at 45 kV at 40 mA. Scans ranged between 5º and 125º at 0.02º increments. Data were processed using Phillips HighScore Plus software. Phase identification by peak comparison was performed using the JCPDS PDF-2 200 powder diffraction database. A total of 14 phases were identified and are listed in Table 4.

Comment [JT1]: Silicon or silica?

Tables 3 and 4 show that both LLNL and COMENA identified the primary phases of quartz, feldspar minerals (albite, anorthite, microcline, orthoclase), and micas (muscovite and chloritoid), consistent with a typical silicate soil. LLNL also identified montmorillonite, a common clay mineral and titanium dioxide, a common accessory mineral. These findings are consistent with a

previously published analysis of IAEA-326 which identified quartz, feldspars, micas, clay, iron oxides, and number of accessory minerals (Bojanowski et al, 2001).

In addition, COMENA identified a number of unusual minerals, including yttrium, nickel, cadmium, copper, gallium, tellurium, and selenium minerals, several hydrated phases, a zeolite, soluble chlorides, and multiple organic compounds. While previous analyses of IAEA-326 reports that humics comprise nearly 6% of the soils, many of these other phases are rare, and may require additional assessment and confirmation.

Table 4. Phases identified by XRD analysis (COMENA).

Ref. Code	Score	Compound Name	Scale Factor	Chemical Formula
00-046-1045	53	Quartz, syn	0.222	Si O2
01-074-1227	20	Strontium Oxide	0.013	Sr O
01-084-1944	20	Yttrium Indium Hydroxide	0.009	Y0.25 In0.75 (O H)3
00-010-0031	19	Sodium Aluminum Silicate	0.016	Na4 Al2 Si2 O9
00-001-1098	12	Muscovite	0.095	H2 K Al3 (Si O4)3
01-085-1352	14	Faujasite nickel m-dichlorbenzene	0.007	Ni28.9 Si133 Al59 O384 (H2 O)24
01-079-2331	18	Copper Gallium Telluride	0.030	Cu Ga Te2
00-022-1618	19	N-(p-Chlorophenyl) benzamide	0.019	C13 H10 Cl N O
00-036-0584	15	Strontium Bromide Chloride	0.020	Sr Br1.6 Cl0.4
01-070-2217	13	Cadmium Chloride Hydrate	0.081	Cd Cl2 (H2 O)4
00-042-1399	19	Zinnwaldite-1\ITM\RG	0.023	K (Al Fe Li) (Si3 Al) O10 (O H) F
00-017-0291	15	Zinc Selenate Hydrate	0.086	Zn Se O4 !6 H2 O
00-028-0814	15	Potassium Thorium Molybdenum Oxide	0.021	K4 Th Mo4 O16
00-012-0956	13	Quinone 2,4-dinitrophenylhydrazone	0.008	C12 H8 N4 O5

Discussion of these results included the role of the analyst's choice of data libraries used for peak deconvolution and phase identification, and the role of experience and expertise in interpretation of XRD results. It was generally recognized that data comparisons may be improved in the future with more formalized reporting formats. In addition, reporting of the confidence of library-based data fits could be integrated by both groups, and may provide an objective basis for analyst decisions to report the presence of trace phases if communicating results forward. It was also noted that, while similar phases were observed in both analyzed samples at LLNL, results were not identical despite their derivation from the same parent aliquot. When mineralogical relationships are taken into account, it can be concluded that differences between the two samples captures some combination of material heterogeneity and XRD precision. Thus, these observations again suggest some degree of sample heterogeneity, even at the tens of gram scale.

8. X-ray Fluorescence

XRF is an elemental analysis technique based on photon emission induced by X-ray bombardment of the sample. Typically, when a mixed element sample is analyzed, the emitted spectrum from

the sample is subject to either energy-dispersive or wavelength-dispersive analysis to separate emissions by specific element according to Moseley's Law.

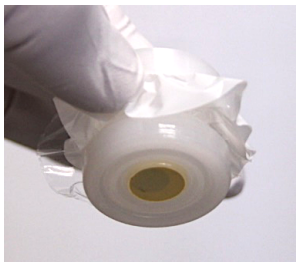

Figure 6. Sample holder used for XRF analysis (LLNL).

LLNL's method of XRF analysis entails loading between 250 and 500 mg of sample powder into a funnel-style sample container. The sample is distributed uniformly on 12 micron thick polypropylene film across an 8 mm orifice, and capped using microporous film (Fig. 6). Samples were analyzed on a Bruker S8 Tiger WD-XRF at 20-60 keV, with PET/LiF200 collimator crystals. All elements ($Z \geq 11$, Na to U) were measured as oxides in semi-quantitative mode using a He atmosphere. Standard glass discs were analyzed to confirm calibration curves, and spectra were screened to assess accuracy of peak ID. Quantitative results were calculated based on measured net intensities using EVAL2 software. Relationships between net intensities and concentrations were determined using the built-in semi-quantitative calibration curve, and concentrations were normalized to 100%, with oxygen calculated by stoichiometry. Uncertainties were determined by replicate analysis of individual samples. The CUP-2 standard (a uranium ore concentrate) was analyzed to assess measurement accuracy for most elements (S, Si, Ti, Ca, V, As, Zr, Fe, Ni, Na, Mo, Mg, K, P). Detection limits for Cu (150 ppm), Fe (100 ppm), Cr (50 ppm), and Ni (50 ppm) are constant due to their presence in the instrument, which creates an invariant background. Results of the sample analyses done at LLNL are provided in Table 5 (left). No significant differences were observed between the major-element contents of the two samples. Slight variations were observed between the minor constituents (Fig. 7).

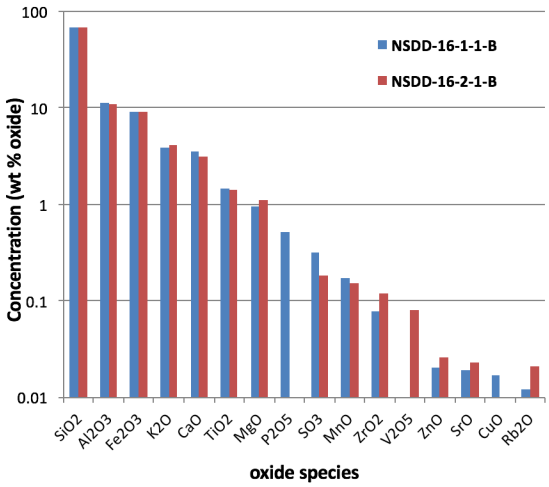

Figure 7. Comparison of the oxide composition of the two samples analyzed by XRF (LLNL) reveal variation in the minor element compositions (oxides present at <1%).

Table 5. XRF analyses (LLNL) and 1σ uncertainties are shown in the table at left. Results are provided calculated as oxides. Note the increase in uncertainties for concentrations <9%. XRF analyses (COMENA) and 1σ uncertainties are shown in the table at right.

	NSDD-16-1-1-B		NSDD-16-2-1-B	
Oxide	Conc.	1σ	Conc.	1σ
SiO2	68.43%	0.96%	69.04%	0.95%
Al2O3	11.35%	2.50%	10.76%	2.55%
Fe2O3	9.15%	0.61%	9.15%	0.60%
K2O	3.91%	1.84%	4.09%	1.78%
CaO	3.50%	2.08%	3.09%	2.18%
TiO2	1.44%	3.17%	1.41%	3.17%
MgO	0.96%	9.84%	1.11%	8.58%
P2O5	0.51%	12.00%	n.d.	
SO3	0.32%	11.30%	0.18%	16.80%
MnO	0.17%	5.94%	0.15%	6.24%
ZrO2	0.08%	2.30%	0.12%	1.84%
V2O5	n.d.		0.08%	11.90%
ZnO	0.02%	14.40%	0.03%	11.50%
SrO	0.02%	6.92%	0.02%	6.71%
CuO	0.02%	18.50%	n.d.	
Rb2O	0.01%	10.00%	0.02%	7.06%

Element	Unit	Concentration
Si	%	32.634 ± 1.850
Al	%	4.401 ± 0.335
Fe	%	2.96 ± 0.08
K	%	1.853 ± 0.106
Ca	%	1.068 ± 0.120
Mg	%	0.862 ± 0.024
Ti	%	0.415 ± 0.024
P	%	0.115 ± 0.009
Mn	ppm	662 ± 42
Ba	ppm	383 ± 31
Zr	ppm	383 ± 22
S	ppm	345 ± 29
Cr	ppm	92.52 ± 6.15
Sr	ppm	91.10 ± 6.37
Rb	ppm	87.65 ± 6.45
V	ppm	83 ± 9
Zn	ppm	72.45 ± 6.55
Y	ppm	40.73 ± 5.86
Cu	ppm	21.3 ± 2.7
Ga	ppm	20.5 ± 3.7
Pb	ppm	19.04 ± 3.32
Nb	ppm	15.20 ± 2.35
Br	ppm	9.71 ± 1.05
Th	ppm	9.48 ± 0.85
Ni	ppm	8.3 ± 1.7
Co	ppm	7.91 ± 1.32
Sc	ppm	7.65 ± 1.91
As	ppm	7.45 ± 1.33
U	ppm	3.53 ± 0.84
Mo	ppm	1.75 ± 0.25

COMENA's XRF analysis compared the performance of two instruments. The primary instrument used was a fixed-laboratory instrument, an Amptek EXP-1 with 40kW source and 1024 channel discriminator (up to 40 keV) and XRS-FP software. The other was a handheld XRF instrument, a Thermo Scientific Niton XL3t. The instruments were cross-calibrated using a number of standards including PTXRF-IAEA-13 (a clay), PTXRF-IAEA-10 (a sandy soil), PTXRF-IAEA-9 (a river clay), PTXRF-IAEA-5 (a marine sediment), PTXRF-IAEA-4 (a clay), WEPAL-ISE41 (a sandy

soil), IAEA Soil-7, SO-3 (Canadian certified reference material[1]), and a blank (a binder comprising 39.7% C, 46.3% O, 4.5% H, 9% Na). For the Amptek instrument, 5 g of sample was analyzed without any prior homogenization. The sample was heated to 105 ˚C for 24 hours to determine moisture content, which was determined to be ~4% by weight. Raw data were inspected to confirm element identification, and software functions used for spectrum smoothing, Si escape peak removal, sum peak removal, background removal, blank removal, and intensity extraction. Reported data can be found in Table 5 (right) and are provided as elemental concentrations. Comparative results from the handheld instrument were not provided as part of the exercise.

If LLNL's results from analysis of two samples are converted to elemental form and compared with COMENA's analysis results, it can be seen that the two approaches arrived at consistent results for the major elements (Table 6). A comparative plot of these major elements also results in a linear regression with a slope of near unity, suggesting the data analyses compare well (Fig. 8). COMENA's low-level results further compare well with LLNL's results, although the latter report larger uncertainties.

Overall, the data comparison is reasonably good given the XRF methodologies and the inherent large uncertainty associated with the results. COMENA identified a number of elements that LLNL did not identify in their spectra, however, including Ba, Cr, Y, Ga, Pb, Nb, Br, Th, Ni, Co, Sc, As, U, and Mo. Discussion centered around confidence in elemental assignments, methods for handling samples with potential heterogeneities, the role that sample matrices may play in the calibration and standardization of instruments, and assignment of uncertainty. In addition, future work looking at comparative analyses between handheld, fixed-laboratory, and dissolution-based elemental concentration methods will be of interest to all.

Table 6. Comparison of COMENA and LLNL's major element results as determined by XRF, with both sets of result reported as elemental percent (by weight).

	NSDD-16-1-1-B, LLNL	1σ	NSDD-16-2-1-B, LLNL	1σ	COMENA	1σ
Si	31.99	0.31	32.42	0.31	32.63	1.85
Fe	6.40	0.04	6.45	0.04	2.96	0.80
Al	6.01	0.15	5.71	0.15	4.40	0.34
K	3.25	0.06	3.42	0.06	1.85	0.11
Ca	2.50	0.05	2.23	0.05	1.07	0.12
Ti	0.86	0.03	0.85	0.03	0.42	0.02
Mg	0.58	0.06	0.67	0.06	0.86	0.02

[1] http://www.nrcan. gc.ca/mining-materials/certified-reference-materials/certificate-price-list/8117

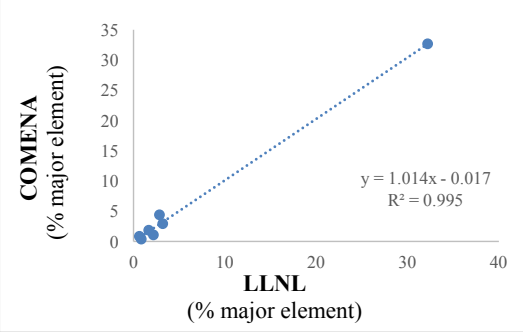

Figure 8. Linear regression of COMENA and LLNL XRF results for the major elements, showing a general one-to-one correlation.

9. Scanning Electron Microscopy

SEM uses a collimated beam of electrons to interact with near-surface electrons through inelastic scattering. This causes secondary electron emission from atomic orbitals, and detectors designed to collect these electrons enable spatial reconstruction of high-resolution morphological images. In addition, backscattered electrons, which are preferentially scattered as a function of average atomic number, can be collected to produce qualitative compositional images. These imaging modes were used by both laboratories to determine particle shape and relative compositional heterogeneity.

LLNL's methods for SEM imaging involved mounting sample particles onto conductive stubs coated with a carbon adhesive, followed by carbon coating to further enhance electron conductivity of the sample. Imaging was performed using an FEI Inspect F Scanning Electron Microscope operated at 20 kV. Imaging modes used secondary electron capture as well as backscatter detection. In addition, energy dispersive analyses were performed using a Bruker EDS system to semi-quantify major-element compositions of selected grains.

The two mounted samples imaged at LLNL (NSDD-16-1-1-C and NSDD-16-1-2-C) were indistinguishable in collected SEM images (Fig. 9). Grain sizes as large as a few hundreds of microns were observed, as well as many agglomerated grains. The smallest grains were sub-micron in dimension, and often occur adhered to the surfaces of larger grains. Grain morphologies tend to be angular, consistent with crushed rock minerals produced by directed crushing (rather than natural causes). No apparent tool marks were observed on any grain surfaces suggesting the use of milling to achieve the resultant particle size. Energy dispersive spectrometry, which interprets the energies of characteristic electrons by element, confirmed the dominance of quartz and feldspars, as well as the presence of Al, Fe, Mg, Ti and Zn-rich oxides. Sodium was observed but only in trace quantities (<0.3%). Many smaller (sub-micron) grains appeared to be iron oxides.

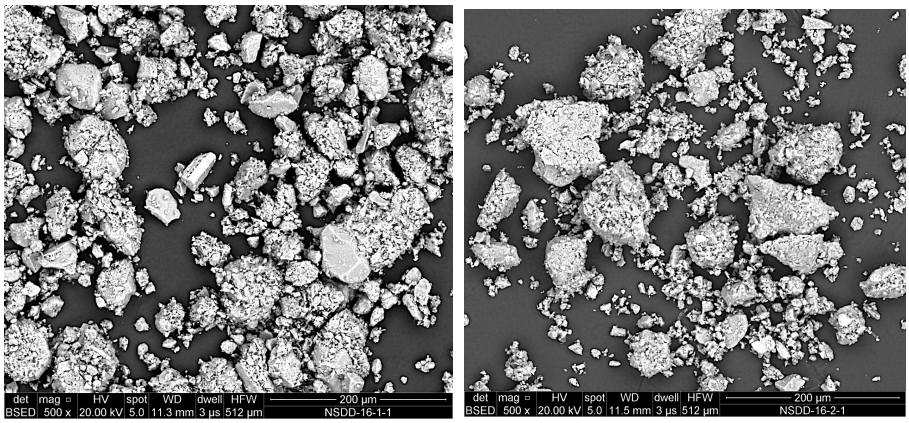

Figure 9. Backscattered electron images of the two samples analyzed at LLNL show a range of grain sizes, with morphologies dominated by angular fragments tens of microns in dimension, with abundant sub-micron grains adhering to the larger grain surfaces.

SEM imaging performed at COMENA used an environmental SEM, which is designed to produce electron images under lower vacuum conditions that those needed for conventional SEM. The analyzed sample was manually mixed prior to analysis. Particles were then dispersed onto double sided carbon tape adhered to a conductive stub (similar to that used by LLNL) to enhance conductivity. Analysis included imaging by both secondary electrons and backscattered electrons, and was performed using a Philips XL30 ESEM FEG Environmental SEM.

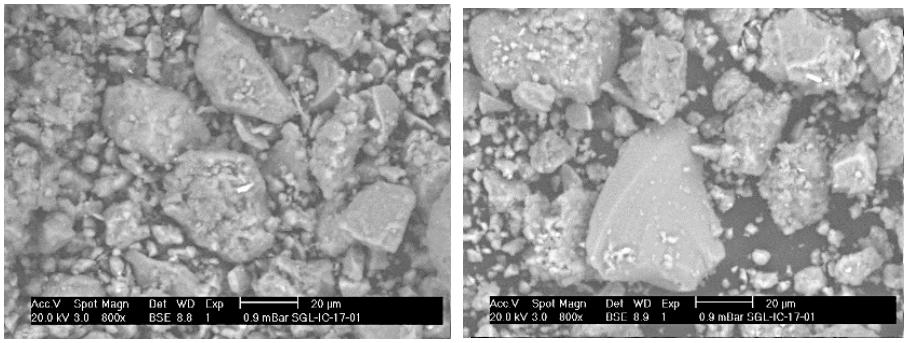

Figure 10. Backscattered electron images collected by COMENA.

Soil particles were described as having a generally spherical shape and ranged in size from a few microns to a few hundred microns, with the majority of particles ~10 µm in dimension (Fig. 10).

Discussion of results centered around the need for consistent lexicons in describing sample morphologies, e.g. similar fragments being described as "angular" vs. "generally spherical" and the role that particle size distribution determination can play in more quantitatively describing particulate samples. Both of these topics are areas of active discussion in the nuclear forensics community. Neither laboratory performed quantitative particle size distribution analyses for this exercise. Discussions also touched on the use of energy-dispersive spectrometry as a method that can be used to provide additional confidence in elemental characterization conducted by other methods such as XRF.

10. Gamma Spectrometry

Gamma spectrometry is used to detect and quantify gamma-emitting radioactivity. For this exercise, all three laboratories used high-purity germanium (HPGe) gamma detectors in a shielded counting chamber. Gamma emissions from a sample are captured by the detector, registering a current that is energy discriminated using a multichannel analyzer. In order to provide quantitative results, the efficiency of the detector has to be determined for each energy of interest, and will vary with the mass and geometry of the sample. All three laboratories performed γ-spectrometry measurements, enabling thorough cross comparison between approaches.

Table 7. Gamma spectrometry for two samples counted by HPGe (LLNL). Uncertainties are 1σ, and include uncertainty propagated from peak fitting, counting statistics, and an estimated 5% relative uncertainty in geometry modelling.

NSDD-16-1-1-D					
Nuclide	Bq/g	1σ*	atoms/g	1σ	pCi/g
^{40}K	0.530	0.053	3.0E+16	3.0E+15	14.3
^{137}Cs	0.111	0.007	1.5E+08	9.5E+06	3.0
^{226}Ra	0.035	0.004	2.6E+09	2.9E+08	1.0
^{228}Th	0.043	0.004	3.7E+06	3.4E+05	1.2
^{232}Th (^{228}Ac)	0.049	0.003	3.1E+16	1.9E+15	1.3
NSDD-16-1-2-D					
Nuclide	Bq/g	1σ*	atoms/g	1σ	pCi/g
^{40}K	0.549	0.050	3.1E+16	2.8E+15	14.8
^{137}Cs	0.102	0.006	1.4E+08	8.4E+06	2.7
^{226}Ra	0.028	0.004	2.1E+09	2.6E+08	0.8
^{228}Th	0.038	0.006	3.3E+06	5.4E+05	1.0
^{232}Th (^{228}Ac)	0.050	0.006	3.2E+16	3.8E+15	1.3

LLNL's method of measuring gamma activity involved collecting data on an Ortec GEM p-type HPGe detector (14% relative efficiency) and Ortec D-Spec electronics. Count time for the samples was 7200 minutes at 4.62 cm from the detector. The two samples were 7.80 g and 9.18 g dry powders, respectively, and both were counted in cylindrical polypropylene vials (3.5 cm diameter x 6.5 cm high). Efficiency calibration, peak fitting, and nuclide identification used Gamanal software and a manual review. Semi-annual point-source efficiency calibrations, regular QC checks and background counts are performed on the instrument. Results of the LLNL sample analyses are presented in Table 7.

LANL's approach to gamma spectrometry takes advantage of an operational system that undergoes daily background checks and ^{152}Eu standard measurements. Control charts are produced each day at different energy levels to quantify instrument drift, and indicate the need for detector maintenance and recalibration. A standard count time for production runs is 1000 minutes, with long counts of 3000 minutes available when needed. All samples are analyzed in a "puck" geometry using a standardized cylindrical shape. In addition to the exercise samples, a contaminated river sediment standard (Columbia River sediment SRM 4350B[2]) was analyzed. Results from LANL's gamma spectrometry are presented in Table 8.

In addition to the ^{137}Cs gamma line at 662 keV, LANL's sample spectra revealed gamma lines at 911 keV (^{228}Ac) and 1461 keV (^{40}K). Signatures of these naturally occurring radionuclides are routinely observed in background spectra; quantification of these materials in the soil sample would therefore require background subtraction, not conducted for this exercise. LANL did not detect any ^{235}U in the samples by gamma spectroscopy, and determined their own ^{235}U detection limits for these samples, using the observed spectrum background in the vicinity of ^{235}U's 185 keV line. ^{235}U detection limits for the two samples were calculated as 0.011 and 0.016 Bq/kg (critical level L_C, 95% confidence).

Table 8. ^{137}Cs results from gamma spectrometry analysis of the two powder samples (LANL), as well as results from the relevant standard analysis (SRM 4350B). Reported errors include only counting statistics.

Sample	LANL 1000-Minute Count 1 (Bq/g)	LANL 1000-Minute Count 2 (Bq/g)	LANL 3000-Minute Count (Bq/g)	NIST Reference (Bq/g)
NSDD 16-1	1.18E-01 (5.8%)	1.18E-01 (4.2%)	1.16E-01 (3.0%)	*n/a*
NSDD 16-2	1.26E-01 (5.2%)	1.25E-01 (5.1%)	1.27E-01 (3.3%)	*n/a*
SRM 4350B	2.03E-02 (16.2%)	1.66E-02 (12.2%)	1.34E-02 (8.1%)	1.27E-02 (6.3%)

[2] https://nemo.nist.gov/srmors/view_detail.cfm?srm=4350B

COMENA's gamma spectrometry analysis also used HPGe gamma counting. The laboratory has a long history of measuring a variety of environmental samples and has participated in many laboratory inter-comparison exercises. They have established detector efficiencies by spiking a sample with both ^{152}Eu and ^{133}Ba, which cover high and low detector energies. Spike concentrations are typically between 1000 and 2000 Bq/50 g. Typically larger mass samples are spiked to measure efficiency as a function of mass, relevant at energy levels below 900 keV. For these samples two different aliquots were measured. Gamma spectrometry results are presented in Table 9.

Comment [KK2]: Were these two aliquots the same mass?

In addition, COMENA also has a Safeguards Laboratory used for determining the presence of ^{235}U in materials, and exercised this capability for the inter-laboratory comparison. The Safeguards laboratory received the sample in mid-June. The sample was identified as a low-level radioactive sample using an HM-5 hand held assay probe. Gamma activity was then measured using a HPGe planar geometry detector coupled to an Inspector Multichannel Analyzer (*see* International Nuclear Verification No. 1, 2003). Their analysis showed that the ^{235}U was not detected above their detection limits of between 0.017 and 0.026 Bq/kg. Accordingly, no ^{235}U was identified at or above the counter detection limit.

Table 9. Results gamma spectrometry analysis (HPGe) at COMENA. Uncertainties are estimated at the 1σ level.

Energy of radioelement	A1 (Bq/kg)	A2 (Bq/kg)	Uncertainty
352 (Pb-214)	31	32	5- 10 %
609 (Bi-214)	29	28	5- 10 %
661.6 (Cs-137)	110	111	5- 10 %
911 (Ac228)	45	44	5- 10 %
1460 (K40)	670	652	5- 10 %

All three labs reported ^{137}Cs results, clearly establishing the sample as having a minor, anthropogenic component. LLNL and COMENA both also reported other natural detectable nuclides (^{40}K and ^{228}Ac) in the samples. These results are compared along with ^{137}Cs in Table 10. Also identified by LLNL was ^{226}Ra, which was quantified from a combination of ^{214}Pb and ^{214}Bi gamma lines. COMENA identified ^{214}Pb and ^{214}Bi, as well, but reported these daughter activities, only. LLNL also detected gamma lines from the Th decay chain and used them to estimate the ^{228}Th and ^{232}Th activities in the soils. None of the laboratories observed actinides present beyond natural levels. Both LANL and COMENA quantified the detection limits for ^{235}U, and reported non-detects within these limits. Given the uncertainties in the measurements, results compare

reasonably well. Discrepancies observed between the samples and laboratories may be due, in part, to inhomogeneity in the sample material (noted in previously reported analyses of the sample).

Table 10. Comparative gamma spectroscopy analysis from all three labs (Bq/g). Replicate analyses are shown.

Lab	^{137}Cs		^{40}K		^{228}Ac	
LLNL	0.1108	0.1015	0.5296	0.5489	0.0485	0.0495
LANL	0.117	0.126	na	na	na	na
COMENA	0.110	0.111	0.670	0.652	0.045	0.044

Follow-on discussions centered around potential sample heterogeneity as well as uncertainty quantification and communication (a different approach was used by all three laboratories). The benefit of following up preliminary counting measurements (such as those done by LLNL) or safeguards measurements (such as those performed at COMENA) with longer-term, higher-quality counting approaches was also discussed, particularly when handling low-level samples.

11. Alpha Spectrometry

Alpha spectrometry is useful for identifying and quantifying the presence of alpha emitters, which include many isotopes of higher mass elements such as uranium, plutonium, and thorium, and is a traditional method for delineating the ratio of uranium and plutonium isotopes. Alpha spectrometry can be a nondestructive method, but due to the very short interaction path lengths, solid samples tend to shield alpha emission. Thus, analysis of alpha activity is generally best performed through dissolution followed by chemical separation and the production of thinly plated sources. The method requires a complete digestion of the sample into an acid. The uranium and plutonium are purified using column chromatography followed by precipitation or electroplating of the purified metal onto a substrate. The substrate is placed into an alpha counter under vacuum to enable the charged alpha particles to reach the detector before being adsorbed by air or water. It was requested that LLNL carry out alpha analysis for comparison with future development at COMENA for this exercise.

LLNL's approach to alpha spectrometry included dissolving the sample by acid treatment and microwave digestion. Blanks were processed along with NIST soil standards following the same procedure. Actinide fractions were purified by precipitation, ion exchange, and extraction columns. Purified fractions were then electroplated onto stainless steel disks in sodium sulfate/bisulfate for 91 minutes at a constant 1.5 A current. Samples were counted at least 5 days at 130 mTorr in Ortec AlphaDuo spectrometers, 1 cm from ultra-low background ion-implanted

Si surface barrier detectors (600 mm^2 x 100 µm thick). Spectra were collected with Maestro software, in the 3-8 MeV energy range. Regions of interest were manually selected for integration. Energy calibration is maintained and background spectra are collected quarterly. In addition, blanks are electroplated and counted between samples.

Table 11. Alpha spectroscopy analysis (LLNL). Note that natural atomic abundance of $^{234}U/^{238}U$ is ~5.5 ± 0.1 x 10^{-5}, with natural variation.

Sample	Activity $^{234}U/^{238}U$	± 1σ	Atom $^{234}U/^{238}U$	± 1σ
NSDD-16-1-1-d	0.88	0.09	4.86E-05	4.8E-06
NSDD-16-2-1-d	1.03	0.08	5.64E-05	4.4E-06
NIST 2709	1.03	0.08	5.64E-05	4.2E-06

Results from the alpha counting show that the two samples have a $^{234}U/^{238}U$ consistent with presence of natural (or slightly depleted) uranium (see Table 11). A 5-day count of Pu fractions suggested trace Pu, but results were indeterminate.

12. Conclusions

This exercise provided an opportunity to demonstrate nuclear forensics analytical capabilities at COMENA, LANL, and LLNL, and identified areas that could benefit from future technical exchanges. The comparative nondestructive analysis of a powdered soil sample was also useful to all participating laboratories as a foundation for inter-laboratory comparisons between major nuclear forensic laboratories. The exercise enabled practice of a flow for sample analysis (execution of an analytical plan including analytical sequencing), as well as the flow of information between analysts. Further work to articulate standard operating procedures for different analytical methods, including the use of calibration standards and libraries, as well as optimization of reporting formats for provision of reported data and analytical conclusions will be areas of focus for continued development.

The exercise also highlighted many of the complications that can arise in the case of potentially heterogeneous samples. In the case of the IAEA-326 soil sample used for this exercise, some degree of heterogeneity is also noted in the original IAEA report (particularly with respect to ^{137}Cs distributions) and was captured through the duplicate LLNL analyses as well by the comparative analyses between the laboratories. To some degree, use of replicate analyses (when not sample limited) can provide independent assessment of potential heterogeneities consistent with the reported levels of precision, and should be encouraged when practical. Our next anticipated exercise will permit further opportunities to practice with these types of materials, and will lead to further improvement of methods and best practices.

13. References

Bojanowski, R., Z. Radecki, M.J. Campbell, K.I. Burns, A. Trinkl, Report on the Intercomparison Run for the Determination of Radionuclides in Soils, IAEA-326 and IAEA-327, *IAEA/AL/100*, 2001.

IAEA, Safeguards Techniques and Equipment, *International Nuclear Verification Series No. 1 (Revised)*, 2003.

Parsons-Davis, T., K. Knight, M. Fitzgerald, G. Stone, L. Caldeira, C. Ramon, M. Kristo, 'Application of Modern Autoradiography to Nuclear Forensic Analysis', *J. Forensic Sci.*, *submitted*.